AIP | Applied Physics Letters

First-principles study on negative thermal expansion of PbTiO3

Fangfang Wang, Ying Xie, Jun Chen, Honggang Fu, and Xianran Xing

Citation: Applied Physics Letters **103**, 221901 (2013); doi: 10.1063/1.4833280
View online: http://dx.doi.org/10.1063/1.4833280
View Table of Contents: http://scitation.aip.org/content/aip/journal/apl/103/22?ver=pdfcov
Published by the AIP Publishing

First-principles study on negative thermal expansion of $PbTiO_3$

Fangfang Wang,[1] Ying Xie,[2] Jun Chen,[1] Honggang Fu,[2] and Xianran Xing[1,a)]
[1]*Department of Physical Chemistry, University of Science and Technology Beijing, Beijing 100083, China*
[2]*Key Laboratory of Functional Inorganic Material Chemistry, Ministry of Education of the People's Republic of China, Heilongjiang University, Harbin 150080, China*

(Received 3 September 2013; accepted 10 November 2013; published online 25 November 2013)

It is well known that perovskite-type $PbTiO_3$ behaves negative thermal expansion in a wide temperature range from room temperature to Curie temperature (763 K). The present study reports the first-principles study of the anisotropic thermal expansion of $PbTiO_3$, in the framework of the density-functional theory and the density-functional perturbation theory. The curve of temperature dependence of the unit cell volume is presented from 20 to 520 K through the calculation of the minimum of total free energy at each temperature point. The negative thermal expansion of $PbTiO_3$ is calculated without empirical parameters. Furthermore, the distinctive thermodynamic act of $PbTiO_3$ from expanding to contracting at tetragonal phase is reproduced. The *ab-initio* calculations reveal that this unique appearance depends on the phonon vibration. The dynamical contributions of various atoms are also calculated to account for the disparate role of Pb-O and Ti-O bond. © *2013 AIP Publishing LLC*. [http://dx.doi.org/10.1063/1.4833280]

Great fundamental and applied interest is generated in the family of perovskite-type materials since these compounds exhibit a wealth of intriguing physical effects.[1] As a ferroelectric prototype, $PbTiO_3$ has drawn much attention. It has a fairly high Curie temperature $T_C = 763$ K, above which it shows a cubic phase. And below 763 K, $PbTiO_3$ shows a tetragonal phase (see the inset of Fig. 2).[2,3] At room temperature (RT), $PbTiO_3$ has a large spontaneous polarization along c axis with c/a ratio = 1.064.[4] It is worth mentioning that $PbTiO_3$ exhibits negative thermal expansion (NTE) in a wide temperature range from the T_C to RT. The unit cell volume of $PbTiO_3$ contracts with an average bulk coefficient of thermal expansion ($\bar{\alpha}_v = -1.99 \times 10^{-5}\,K^{-1}$).[5] Interestingly, the thermal expansion is anisotropic. The axis paralleling to polarization direction, i.e., c axis, shrinks rapidly, while the axis which is perpendicular to the polarization direction, i.e., a axis, is expanding as the temperature increases. However, the NTE only happens from RT to T_C. Below RT, $PbTiO_3$ exhibits positive thermal expansion like most of materials. The abnormal behavior of thermal expansion of $PbTiO_3$ raised widespread concerns experimentally. Particularly, our previous works focused on the nature of the NTE behavior of $PbTiO_3$ in the past decade.[5–7] The researches revealed broad prospects for structure and phase transition of $PbTiO_3$. However, in-depth understanding of thermodynamic properties, especially the transformation of the thermal expansion between positive and negative, is still unsolved. To date, we are looking for more efficient theory calculated method to perfect this research.

Nowadays, first-principles calculation has become a powerful tool in materials research.[8–11] In the past two decades, first-principles works on thermal expansion calculations are mostly confined to cubic metals. They have given splendid outcomes about isotropic thermal expansion and related thermal properties.[12–14] However, due to the difficulties in theoretical realization and large computational cost, the *ab-initio* investigation of anisotropic thermal expansion has seldom been touched.[15–17] Furthermore, the research about the NTE of $PbTiO_3$ using first-principles method is scanty. Costa and co-workers performed molecular dynamics simulation for the structural phase transition in $PbTiO_3$, which was reproduced with both temperature and pressure.[18] Yet, their study failed to recur with NTE phenomenon which is observed experimentally.

In this paper, we investigated the anisotropic thermal expansion of $PbTiO_3$ using first-principles calculation coupled with the density functional theory (DFT) and density functional perturbation theory (DFPT).[19,20] We performed 42 sets with different lattice parameters and calculated their energy at different temperatures. At a certain temperature, we could easily compare the energy of 42 sets. As it is well known that the structure with minimum value of energy should be the most stable. Upon this method, the stable structure at different temperatures has been demonstrated. The behavior of thermal expansion is simulated, which matches well the experimental data. We also discussed the thermodynamic properties of this distinctive expansion act and the dynamical contributions of various atoms. Moreover, first-principles method is well applied to the thermal expansion calculation of anisotropy perovskites. It is expected that this method will be used as a guide for the design and forecast of more NTE materials in the future.

To calculate the thermal properties of the investigated materials, we used a plane-wave pseudopotential method based on DFT and DFPT implemented in the code ABINIT.[21] The norm-conserving generalized gradient approximation (GGA) pseudopotentials are generated in the scheme of Troullier–Martins.[22] The calculating parameters were optimized at first. The plane-wave energy cutoff of 40.0 hartree is chosen to guarantee the total-energy error in 0.00001 hartree. Brillouin-zone integrations were performed using $8 \times 8 \times 8$ $\vec{k}$-point mesh, and phonon frequencies were computed on a $4 \times 4 \times 4$ $\vec{q}$-point mesh. In order to make

a)Author to whom correspondence should be addressed. Electronic mail: xing@ustb.edu.cn

way for computational resource-saving, we performed 42 sets of first-principles ground-state and response-function calculations of $PbTiO_3$ by varying lattice parameters as shown in Fig. 1, and each black square denotes one structure model, respectively. The internal freedoms within the unit cell are fully relaxed.

The thermodynamical properties usually depend on the appropriate thermodynamical potential relevant to the given ensemble. The relevant potential, e.g., Helmholtz free energy can be written as the equilibrium structure parameters of the crystal at any temperature. We calculated the full phonon spectrum by the Fourier interpolation algorithm of dynamical matrices.[23] Based on the calculated phonon frequencies, we further derived Helmholtz free energies $F(T)$ as a function of the temperature as follows:[24]

$$F(T) = E_s + \int g(\omega)\left(\frac{\hbar\omega}{2} + k_B T \ln\{1 - e^{-\hbar\omega/(k_B T)}\}\right)d\omega, \tag{1}$$

where E_s refers to the static energy, which is the total energy of the crystal at its equilibrium state; the next term is the lattice vibrational free energy, for which ω is the phonon frequency and $g(\omega)$ is the phonon density of states. In accordance with this function, the lattice vibrational free energy and then the total Helmholtz free energy were calculated.[25] We calculated total free energy of 42 sets at each temperature point from 20 to 600 K with a step of 20 K (Fig. 1). To demonstrate more distinctly, the minimum of all the calculated energy is set to zero.

The contour maps of Helmholtz free energy to lattice parameters show quiet different outcomes with three representative temperatures (120 K, 320 K, and 520 K shown in Figs. 1(a)–1(c)). The parallel and vertical axes are, respectively, along a and c axis, and the energy unit is in hartree. The red and blue regions indicate areas of high energy and low energy, respectively. At each temperature point, the minimum of $F(T)$ is given by the center of the blue region, namely, the most stable lattice parameters. The minimum value of $F(T)$ shifts from the upper left corner (high value of c/a) to the lower right corner ($c/a = 1$) of the figure with increasing temperature. The result is similar to the structure parameters transformation which has measured experimentally.[26] What is more, the variation trend of structure with different temperatures is shown in Fig. 1(d). Meanwhile, the XY surface projection of the trend has been revealed (red curve). It can be seen that the c axis becomes shorter at elevated temperatures, while the a axis turns to be longer. Additionally, the c axis decreases smoothly below 120 K and rapidly above 120 K, while a axis increases steadily at the whole range of temperature.

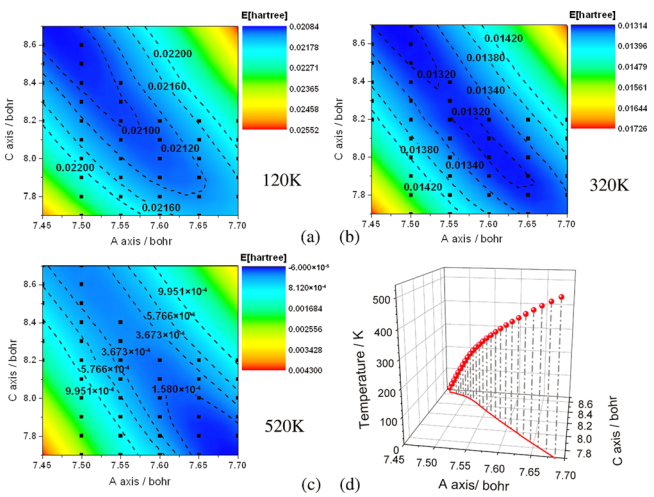

FIG. 1. The contour maps of total Helmholtz free energy at T = 120 K (a), 320 K (b), and 520 K (c). The parallel and vertical axes are, respectively, along a and c axis. The energy unit is in hartree. Red and blue regions indicate areas of high energy and low energy. Black squares denote the structures modeled. The continuous trend of lattice parameters with different temperatures is shown in (d). The red balls indicate different structure at disparate temperatures. The red line denotes XY surface projection of the trend.

After the most stable structure at each temperature point is confirmed, the structure variation of $PbTiO_3$ has been estimated based on the results of first-principles calculations. Figure 2 shows our *ab-initio* results for the temperature dependence of the unit cell volume of $PbTiO_3$. The unit cell volume of $PbTiO_3$ displays positive thermal expansion below 120 K. However, when the temperature rises above 120 K, it contracts gradually until 520 K. What is more, from positive to negative, the thermal expansion process transfers consecutively without any phase transition. It needs to be mentioned that the simulated lattices' parameters are similar to the experimental data.[5] This abnormal behavior of thermal expansion has brought about a crucial concern experimentally since 60 years ago. Shirane *et al.* provided the measurement of the cell parameters of $PbTiO_3$ by X-ray diffraction and revealed that the unit cell volume shrunken with temperature increasing below 763 K.[26,27] Thirty years later, Mabud and Glazer measured the structure parameters of $PbTiO_3$ by a neutron powder diffraction method and found the unit cell volume expands in the temperature range from 180 K to RT.[28] A decade ago, our group re-determined lattice parameters of $PbTiO_3$ in the wide temperature range from 123 K to 1223 K by X-ray diffraction measurements.[5] We observed systematically that $PbTiO_3$ exhibits NTE from RT to T_C, and positive thermal expansion from 123 K to RT and above T_C. Also the research clarified that there is no evidence for phase transition at a relatively low temperature. Afterwards, Costa and co-workers performed molecular dynamics simulation for the structural phase transition in

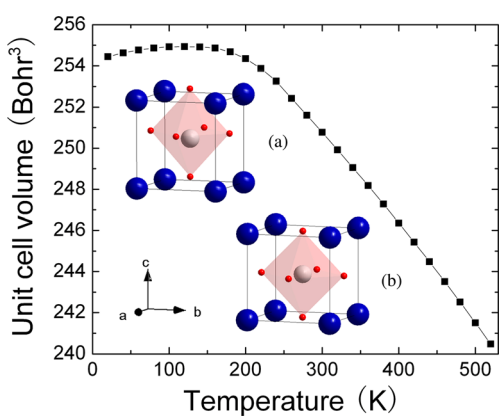

FIG. 2. Temperature dependence of the unit cell volume for $PbTiO_3$. The inset shows crystal structure of (a) tetragonal and (b) cubic $PbTiO_3$. The blue, white, and red balls indicate Pb, Ti, and O atoms, respectively.

$PbTiO_3$.[18] But there is no one yet has calculated the tendency of thermal expansion of $PbTiO_3$ by first-principles from 0 K (unpredictable at experiment) to phase transition temperature. Our calculations predict the thermal expansion from positive to negative and the phase transition from tetragonal to cubic. However, our calculations overestimate the experimental data by Perdew-Burke-Ernzerhof (PBE) functional, which is widespread by first-principles calculations.[29,30] More specifically, the simulated lattice constants a axis is equal to 3.947 Å which overestimates the experimental lattice constant by 1.5% at tetragonal phase.[5] And the simulated tetragonality ($c/a = 1.158$) slightly overestimates the experimental tetragonality ($c/a = 1.071$), in comparison to tetragonality ($c/a = 1.221$) by fully relaxed method.[31] Such a supertetragonality has already been reported for the GGA-PBE functional in the case of $PbTiO_3$.[30,32] Meanwhile, at cubic phase, the simulated lattice constants a axis overestimates the experimental one by 2.1%. And the vibrational free energy in this report is obtained using the quasiharmonic approximation. Undoubtedly, the result would be more reasonable if we take the anharmonic effects into account. Thus, a combination of these two effects leads to aggravated errors.

To make out the physical significance of positive and negative processes of thermal expansion, the contour maps of total Helmholtz free energy have been decomposed into two aspects contributions: static energy and vibrational energy. The contour maps of vibrational free energy at different temperatures are carried out (see Figs. 3(a)–3(d)) by first-principles response function and ground-state methods. White line represents the tendency of lattice parameters of $PbTiO_3$, and the black arrow denotes the energy gradient descent direction. The energy gradient descent direction indicates structure distortion trend generated by lattice vibration here. Meanwhile, the contour map of static energy is shown in Fig. 3(e), which is established by electronic interaction. Without considering the influence of temperature, the electronic contribution keeps the structure of $PbTiO_3$ located at a longer c axis and a shorter a axis. As the temperature rises, the stable structure is distorted due to the introduction of vibration energy. Around 20 K, the effect of vibrational free energy on structure impels both longer a and c, and thus the volume exhibits a thermal expansion (Fig. 3(a)). However, the vibrational free energy converts the arrow as temperature increases, which brings about a longer a axis and a shorter c axis at a relatively high temperature, i.e., 520 K (Fig. 3(d)). Certainly, vibrational free energy is contributed from thermal vibration, while the static energy is established by electronic interaction without considering temperature. The equilibrium lattice parameters are obtained by the balance of thermal vibration favoring cubic phase and electronic interaction favoring ferroelectric (Fig. 3(f)). But due to their different proportion of contribution to the total free energy, their curve is not symmetrical. Combining thermal vibration and electronic interaction, the unit cell volume undergoes the process from expansion to contraction.

Following Eq. (1), we learned that the lattice vibrational free energy is influenced by the phonon frequency ω and the phonon density of states $g(\omega)$. In order to distinguish the dynamical contributions of various atoms, we calculated the

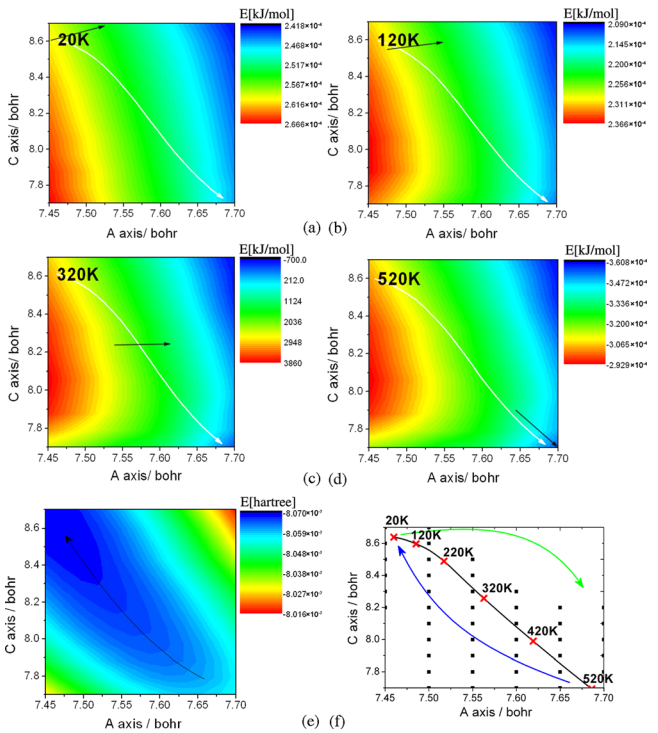

FIG. 3. The contour maps of vibrational free energy at T = 20 K (a), 120 K (b), 320 K (c), and 520 K (d). White line represents the tendency of lattice parameters of $PbTiO_3$. The contour map of the static energy is shown in (e). The continuous trends of the static energy (blue line), vibrational free (green line), and total free energy (black line) with different temperatures is shown in (f). The parallel and vertical axes are, respectively, along a and c axis. Red and blue regions indicate areas of high energy and low energy, respectively. Black squares denote the structures modeled. The black arrow denotes the energy gradient descent direction.

partial phonon density of states. One representation is given in Fig. 4 at $a = 7.5$ bohrs and $c = 8.6$ bohrs. The result matches well the pervious experimental and calculated data.[33] Pb-O bonding character contributes the low frequency vibrations (0 to 100 cm^{-1}), while Ti-O bonds are located at high frequency vibrations. Next, we decomposed the vibrational energy into three parts: the contributions of Pb, Ti, and O atoms. At different temperatures, their contributions to vibrational free energy are calculated using the second term of Eq. (1). The contour maps of the three atoms vibrational free energy at 20 K and 520 K are shown in Fig. 5. White line represents the tendency of lattice

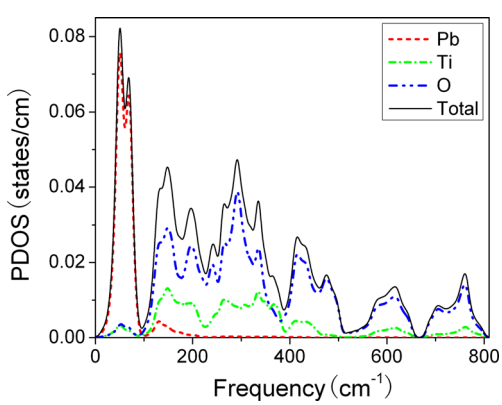

FIG. 4. The computed total and partial phonon densities of states of $PbTiO_3$ at $a = 7.5$ bohrs and $c = 8.6$ bohrs.

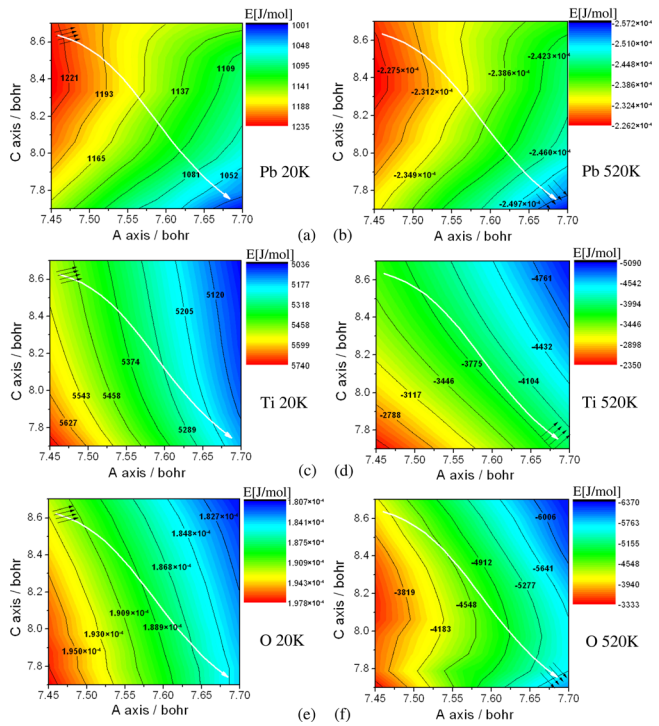

FIG. 5. The contour maps of vibrational free energy of various atoms at T = 20 K and 520 K. White line represents the tendency of lattice parameters of $PbTiO_3$. The parallel and vertical axes are, respectively, along *a* and *c* axis. The energy unit is in kJ/mol. Red and blue regions indicate areas of high energy and low energy, respectively. The black arrow denotes the energy gradient descent direction.

parameters of $PbTiO_3$ as calculated above. And the black arrow denotes the energy gradient descent direction. At a relatively low temperature, the energy descent direction of three atoms is accordant, expanding the structure. It is obvious that the energy interval of Ti and O atoms is wider than Pb atoms, which demonstrates that Ti-O bonding plays a dominant role at a relatively low temperature in terms of vibration energy. As the temperature increases, the energy descent direction of Ti atoms remains unchanged. Nevertheless, the energy gradient of Pb and O atoms forces *c* axis to be shorter. And dissimilar to low temperature, Pb-O bonding plays a key role at a relatively high temperature because of the energy level. Therefore, the thermal vibration of Pb and O atoms causes $PbTiO_3$ favoring cubic phase with increasing temperature. This coincides with the previous outcomes. $PbTiO_3$ is *A*-site driven, while some classic ferroelectric perovskites as $BaTiO_3$ and $KNbO_3$ are *B*-site driven.[8,34] Ti distortion is unfavorable in $PbTiO_3$ in the absence of Pb displacement.[35] Plenty of researches launched around the view that electronic contribution in $PbTiO_3$ should be attributed to hybridization of Pb 6*s* and O 2*p* at a low temperature.[34] This hybridization stabilizes the tetragonal phase. As the temperature increases, the thermal vibration of Pb and O atoms plays an increasingly vital role which destroys the hybridization between Pb-O bonds since the thermal vibration of Pb and O atoms favors cubic phase. And when the temperature increases to T_C, $PbTiO_3$ converts into cubic phase. To summarize, the Pb-O bond keeps tetragonal phase at a low temperature. That the thermal vibration of Pb-O bond favoring the cubic phase destroys the tetragonal phase. The competition process causes NTE of $PbTiO_3$ from RT to T_C. And Ti-O bonding is the reason of positive thermal expansion at a low temperature. With the combined actions between the thermal vibration of Ti-O and Pb-O bonds, $PbTiO_3$ exhibits thermal expansion from positive to negative.

To sum up, we have performed the first-principles calculation for the structural and thermodynamic properties of $PbTiO_3$ by the DFT and DFPT. By calculating the Helmholtz free energy, temperature dependences of the unit cell volume of $PbTiO_3$ has been described, which is similar to the experimentally measured value. The NTE of $PbTiO_3$ is calculated without empirical parameters. Furthermore, the transformation from expansion to contraction is observed by simulating the volume change, which is highly correlated to the phonon thermal vibration. The vibrational free energy of Pb, Ti and O atoms is calculated to analyze the contribution to the volume change of the various atoms. Ti-O bond drives the unit cell volume to expand at the whole temperature range. However, thermal vibration of Pb-O bond destroys the hybridization between Pb and O atoms and favors cubic phase with increasing temperature. Consequently, $PbTiO_3$ exhibits the unusual behavior of thermal expansion with the combination of Pb-O and Ti-O bond.

This work was financially supported by the National Natural Science Foundation of China (Nos. 21231001, 21031005, and 91022016) and Program for Changjiang Scholars and Innovative Research Team in University (No. IRT1207). The calculations were performed on the Quantum Materials Simulator of USTB.

[1]G. H. Haertling, J. Am. Ceram. Soc. **82**, 797–818 (1999).
[2]V. G. Koukhar, N. A. Pertsev, and R. Waser, Phys. Rev. B **64**, 214103 (2001).
[3]M. Budimir, D. Damjanovic, and N. Setter, Phys. Rev. B **72**, 064107 (2005).
[4]W. L. Zhong, B. Jiang, P. L. Zhang, J. M. Ma, H. M. Cheng, and Z. H. Yang, J. Phys.: Condens. Matter **5**, 2619 (1993).
[5]X. R. Xing, J. X. Deng, J. Chen, and G. R. Liu, Rare Met. **22**, 294 (2003).
[6]J. Chen, X. R. Xing, C. Sun, P. H. Hu, R. B. Yu, X. W. Wang, and L. H. Li, J. Am. Chem. Soc. **130**, 1144 (2008).
[7]J. Chen, K. Nittala, J. S. Forrester, J. L. Jones, J. X. Deng, R. B. Yu, and X. R. Xing, J. Am. Chem. Soc. **133**, 11114 (2011).
[8]W. Zhong, D. Vanderbilt, and K. M. Rabe, Phys. Rev. Lett. **73**, 1861 (1994).
[9]I. A. Kornev, L. Bellaiche, P.-E. Janolin, B. Dkhil, and E. Suard, Phys. Rev. Lett. **97**, 157601 (2006).
[10]I. Grinberg and A. M. Rappe, Phase Transitions **80**, 351–368 (2007).
[11]P. Ganesh and R. E. Cohen, J. Phys.: Condens. Matter **21**, 064225 (2009).
[12]J. Xie, S. de Gironcoli, S. Baroni, and M. Scheffler, Phys. Rev. B **59**, 965 (1999).
[13]S. Narasimhan and S. de Gironcoli, Phys. Rev. B **65**, 064302 (2002).
[14]D. N. Talwar, G. Thaler, S. Zaranek, K. Peterson, S. Linger, D. Walker, and K. Holliday, Phys. Rev. B **55**, 11293 (1997).
[15]S. Q. Wang, Appl. Phys. Lett. **88**, 061902 (2006).
[16]Y. Z. Nie, Y. Q. Xie, X. B. Li, and H. J. Peng, J. Phys. Chem. Solids **69**, 852 (2008).
[17]P. Souvatzis, O. Eriksson, and M. I. Katsnelson, Phys. Rev. Lett. **99**, 015901 (2007).
[18]S. C. Costa, P. S. Pizani, J. P. Rino, and D. S. Borges, J. Phys.: Condens. Matter **17**, 5771 (2005).
[19]X. Gonze, Phys. Rev. B **55**, 10337 (1997).
[20]S. Q. Wang and H. Q. Ye, J. Phys.: Condens. Matter **17**, 4475 (2005).
[21]X. Gonze, J.-M. Beuken, R. Caracas, F. Detraux, and M. Fuchs, Comput. Mater. Sci. **25**, 478 (2002).
[22]N. Troullier and J. L. Martins, Phys. Rev. B **43**, 1993 (1991).

[23]S. Baroni, S. de Gironcoli, A. D. Corso, and P. Giannozzi, Rev. Mod. Phys. **73**, 515 (2001).
[24]X.-Q. Chen, W. Wolf, R. Podloucky, and P. Rogl, Phys. Rev. B **71**, 174101 (2005).
[25]C. Lee and X. Gonze, Phys. Rev. B **51**, 8610 (1995).
[26]G. Shirane and S. Hoshino, J. Phys. Soc. Jpn. **6**, 265 (1951).
[27]G. Shirane, K. Suzuki, and A. Takeda, J. Phys. Soc. Jpn. **7**, 12 (1952).
[28]S. A. Mabud and A. M. Glazer, J. Appl. Crystallogr. **12**, 49 (1979).
[29]I. Hamdi and N. Meskini, Physica B **405**, 2785 (2010).
[30]J. P. Perdew, K. Burke, and M. Ernzerhof, Phys. Rev. Lett. **77**, 3865 (1996).
[31]D. I. Bilc, R. Orlando, R. Shaltaf, G.-M. Rignanese, J. Íñiguez, and Ph. Ghosez, Phys. Rev. B **77**, 165107 (2008).
[32]G. Kern, G. Kresse, and J. Hafner, Phys. Rev. B **59**, 8551 (1999).
[33]N. Choudhury, E. J. Walter, A. I. Kolesnikov, and C.-K. Loong, Phys. Rev. B **77**, 134111 (2008).
[34]R. E. Cohen, Nature **358**, 136 (1992).
[35]Ph. Ghosez, E. Cockayne, U. V. Waghmare, and K. M. Rabe, Phys. Rev. B **60**, 836 (1999).